

Hard Negative Samples Emphasis Tracker without Anchors

Zhongzhou Zhang

School of Microelectronics and Communication
Engineering, Chongqing University, China
zz.zhang@cqu.edu.cn

Lei Zhang*

School of Microelectronics and Communication
Engineering, Chongqing University, China
leizhang@cqu.edu.cn

ABSTRACT

Trackers based on Siamese network have shown tremendous success, because of their balance between accuracy and speed. Nevertheless, with tracking scenarios becoming more and more sophisticated, most existing Siamese-based approaches ignore the addressing of the problem that distinguishes the tracking target from hard negative samples in the tracking phase. The features learned by these networks lack of discrimination, which significantly weakens the robustness of Siamese-based trackers and leads to suboptimal performance. To address this issue, we propose a simple yet efficient hard negative samples emphasis method, which constrains Siamese network to learn features that are aware of hard negative samples and enhance the discrimination of embedding features. Through a distance constraint, we force to shorten the distance between exemplar vector and positive vectors, meanwhile, enlarge the distance between exemplar vector and hard negative vectors. Furthermore, we explore a novel anchor-free tracking framework in a per-pixel prediction fashion, which can significantly reduce the number of hyper-parameters and simplify the tracking process by taking full advantage of the representation of convolutional neural network. Extensive experiments on six standard benchmark datasets demonstrate that the proposed method can perform favorable results against state-of-the-art approaches.

CCS CONCEPTS

• Computing methodologies → Tracking; Computer vision.

KEYWORDS

Visual Tracking; Siamese Network; Hard Negative Samples; Anchor-free Tracker

ACM Reference Format:

Zhongzhou Zhang and Lei Zhang. 2020. Hard Negative Samples Emphasis Tracker without Anchors. In *Proceedings of the 28th ACM International Conference on Multimedia (MM '20)*, October 12–16, 2020, Seattle, WA, USA. ACM, New York, NY, USA, 9 pages. <https://doi.org/10.1145/3394171.3413692>

*Corresponding author.

Permission to make digital or hard copies of all or part of this work for personal or classroom use is granted without fee provided that copies are not made or distributed for profit or commercial advantage and that copies bear this notice and the full citation on the first page. Copyrights for components of this work owned by others than ACM must be honored. Abstracting with credit is permitted. To copy otherwise, or republish, to post on servers or to redistribute to lists, requires prior specific permission and/or a fee. Request permissions from permissions@acm.org.

MM '20, October 12–16, 2020, Seattle, WA, USA

© 2020 Association for Computing Machinery.

ACM ISBN 978-1-4503-7988-5/20/10...\$15.00

<https://doi.org/10.1145/3394171.3413692>

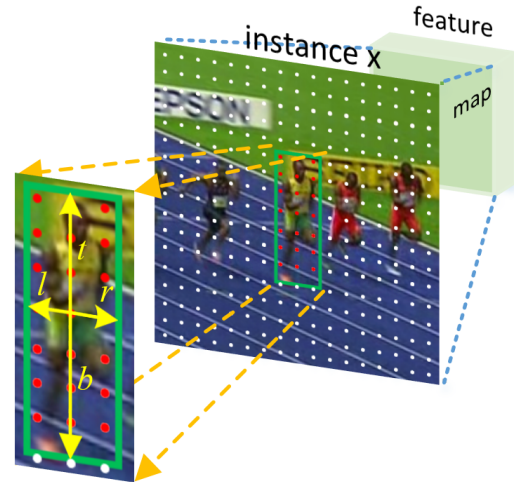


Figure 1: Instantiation of pre-pixel prediction fashion. We map the points in the feature map back to the instance x . Points in red inside ground-truth (the green box) represent positive samples and points in white denote negative samples. Narrows in yellow denote the regression targets (l^*, t^*, r^*, b^*).

1 INTRODUCTION

Visual object tracking is one of the fundamental computer vision problems, which aims to estimate the trajectory of an arbitrary visual target when only an initial state of the target is available. Generic visual tracking is a sought-after yet challenging research topic with a wide range of applications, such as self-driving cars, surveillance, augmented reality, unmanned aerial vehicles, to name a few [42, 43]. Although much progress has been achieved in recent years, it remains a challenge to design robust trackers due to many factors including occlusion, out-of-view, deformation, background cluster, motion blur and so on.

Recently, Siamese-based trackers [9, 23, 24, 41, 50] have drawn great attention in visual tracking community by achieving favorable performance and high efficiency. One representative example is SiamFC [1], which learns similarity knowledge of the same object in different frames in an end-to-end off-line training method. SiamFC [1] simply adopts multi-scale search to estimate the target scale. To get bounding box with different aspect ratios, Siamese-RPN [24] integrates Siamese subnetwork and region proposal subnetwork (RPN) [35]. By using pre-defined anchor boxes with different scales and aspect ratios, Siamese-RPN [24] can predict more accurate bounding boxes. Although they have obtained good performance, there are still some problems that should be addressed. (1) Anchor-based

trackers bring many additional hyper-parameters, such as the number of pre-defined anchors. For a tracking task, speed is also an important indicator in practical applications. Too many pre-defined anchors severely reduce computational efficiency. (2) Most Siamese-based approaches ignore to address the problem of distinguishing positive samples from hard negative samples in the tracking phase. Actually, all samples of the search images can be categorized into three types: *positive samples*, *easy negative samples* and *hard negative samples*. Positive samples are samples that near the center of the tracking target. Easy negative samples include non-semantic background and samples that are not similar to the tracking target. Compared with those easy negative samples, hard negative samples means those samples belonging to the same class of the tracking target, which are similar to positive samples in some tracking sequences. Because there is no effective means to eliminate the effect of hard negative samples, it is difficult for most Siamese-based trackers [1, 9, 23, 24, 41, 50] to distinguish positive samples from hard negative samples during tracking. Furthermore, the number of negative samples is much more than that of positive samples, so the imbalance from positive samples and negative samples also hinder better performance of Siamese-based approaches.

To solve the aforementioned problems, we first put forward an anchor-free tracking method with a per-pixel prediction fashion and the architecture is carefully designed for an end-to-end training manner. Both classification branch and regression branch in FCOS [39] head are designed for foreground-background classification and bounding box prediction respectively. Different from anchor-based methods, the regression target of our tracker is 4D vectors that denote the distances from points within ground-truth to the four sides of the ground-truth bounding box. As illustrated in Figure 1. It is capable of obtaining the coordinate of tracking target and a precise bounding box, which do not need many pre-defined anchors. In this way, our method can not only reduce the number of hyper-parameters but also improve the computational efficiency.

Besides, we propose a hard negative samples emphasis method, which can effectively constrain hard negative samples. General Siamese-based trackers localize the tracking target by finding the coordinate of the maximum value in the score map. However, hard negative samples also have large score responses, leading to tracking failures. To handle this problem, we can select some candidates that include positive samples and hard negative samples, according to the ranking values in the score map. Non-Maximum Suppression (NMS) [35] is adopted to filter out redundant bounding boxes. These selected samples can be classified into positive samples and hard negative samples by their IoU values with the ground-truth. Taking inspiration from person re-identification, we employ a contrastive loss to enlarge the distances between positive samples and hard negative samples. Also, an operation of random shifts of the ground-truth is introduced to keep the balance between positive samples and hard negative samples. The main contributions of this work are summarized as the following threefold:

- We explore a new anchor-free tracking method that adopts pre-pixel prediction fashion to get accurate bounding boxes. And our method can reduce hyper-parameters and improve computational efficiency.

- We propose a novel hard negative samples emphasis method to overcome the weak distinguishability between positive samples and hard negative samples.
- We extensively evaluate the proposed method on six benchmark datasets including GOT-10k [16], UAV123 [31], VOT2016 [18], VOT2018 [19], VOT2019 [20], LaSOT [8]. Our method performs well against state-of-the-art trackers.

2 RELATED WORK

Siamese Network for Tracking. Siamese network trained with similarity learning strategy is first applied in face verification. With the development of deep learning, representative networks are introduced in the tracking community. SINT [38] explores Siamese network to the tracking problem, which implements two-stream Convolution Neural Networks(CNNs) with shared parameters to learning a match function in the off-line training phase. During on-line tracking, it searches for the candidate’s position in the search region by the exemplar that is obtained from the first frame. However, slow speed hinders the development of SINT. After that, Bertinetto et al. [1] put forward fully convolutional Siamese network, namely SiamFC, which significantly improves the tracking speed with 86 FPS on a single GPU. SiamFC [1] is trained by large-scale image pairs to learn a similarity function in an end-to-end manner. Inspired by Faster RCNN [14], Siamese-RPN [24] integrates Siamese network with region proposal network (RPN) to obtain more accurate bounding boxes. Siamese-RPN [24] performs a classification branch and a regression branch. Previous mentioned Siamese-based trackers almost take AlexNet [21] as their backbone for feature extraction. Directly using modern deep neural networks including VGG [36], ResNet [14], Inception [37] into Siamese-based trackers brings about severe decrease of tracking performance. To deal with this issue, Li et al. [24] introduce an effective sampling method to alleviate the impact of padding operation in the training phase. Furthermore, a depth-wise cross-correlation operation [23] is proposed to reduce the computational cost and enhance the representation of feature maps. Zhang et al. [50] present a detailed study of factors that affect tracking performance. Based on their conclusions, they design new deeper and wider networks that are specifically used for Siamese-based trackers. Many Siamese-based trackers borrow modules or designs from object detection community. For example, SPM-tracker [41] designs a two-stage network, namely coarse matching stage and fine matching stage, which can achieve high localization precision. C-RPN [9] adopts a multi-stage tracking framework with three RPNs cascaded and leverages features of different levels, which capable of getting remarkable performance.

Anchor-free Object Detection. Object detection and object tracking have some common similarities like the RPN module mentioned earlier. Anchor-free detection methods have not been explored in the tracking community. YOLOv1 [34] is the well-known anchor-free detector, which predicts bounding boxes relying on grid cells and the grid cells are generated by input images. CornerNet [22] introduces a new one-stage approach to object detection that detects an object as a pair of key points, the top-left corner and the bottom-right corner of bounding boxes. Recently, Tian et al. [39] proposes a full convolutional one-stage object detection (FCOS),

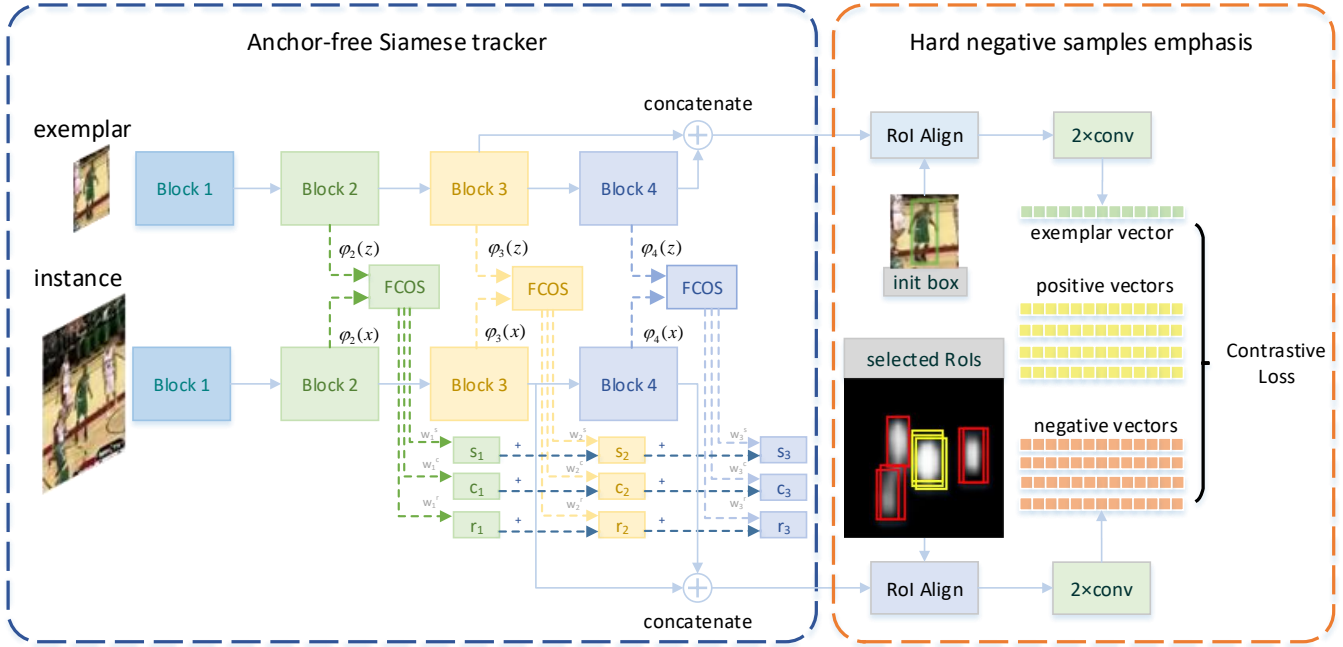


Figure 2: Overview of the proposed framework. Our anchor-free Siamese tracker employs modified ResNet-50 [14] as backbone for extracting multi-level features. Multi-level features are taken as the inputs of FCOS heads for score map (s), center-ness (c) and regression (r). Then RoI Align layer takes selected RoIs and concatenated features as input to obtain pooled features. Two convolutional layers are performed to make the pooled features become vectors. Finally, we adopt a contrastive loss to constrain hard negative samples.

which gets remarkable performance on MSCOCO [30] benchmark. They explore a per-pixel bounding box prediction fashion. By omitting a huge number of anchors, FCOS [39] significantly reduces hyper-parameters and avoids complicated computation.

3 THE PROPOSED TRACKER

We first develop an anchor-free Siamese tracker for foreground-background classification and accurate bounding box prediction in detail. The proposed tracker adopts a per-pixel prediction fashion, which takes the distances from the location of a positive sample to the four sides of the ground-truth bounding box as its regression targets. Furthermore, to tackle the problem caused by hard negative samples, we explore a hard negative samples emphasis method to maintain the discrimination of positive samples and hard negative samples in the embedding space.

3.1 Deep Siamese Network

In this subsection, we introduce the proposed tracking framework which is illustrated in Figure 2. We adopt the modified ResNet-50 [14] as our backbone for feature extraction. The stride of original ResNet-50 is 32 pixels. To make it better suited for tracking, we adjust the effective strides of block 3 and block 4 from 16 pixels and 32 pixels to 8 pixels by the same strategy as [23]. Our Siamese network consists of two branches, namely exemplar branch and instance branch, which have the same architecture and share network parameters. During training, large-scale cropped template

images (exemplar z) and larger search images (instance x) are sent to exemplar branch and instance branch in pairs, extracting embedding features of exemplar z and instance x . Due to different levels of Siamese network contain high-level and low-level features with diverse feature representations, we intend to leverage multi-level features to take full advantage of semantic information and detailed information. Multi-level features include the outputs of *Block 2*, *Block 3*, *Block 4*. Then, we use a 1×1 convolutional layer to make sure the channels of multi-level features becoming the same. The adjusted features can be expressed as $\varphi_i(z)$ and $\varphi_i(x)$, $i \in \{2, 3, 4\}$.

3.2 Anchor-free Siamese Tracker

Both classification branch and regression branch in FCOS [39] head are designed for localization and bounding box estimation. To be specific, three FCOS heads take multi-level features of exemplar z and instance x as input. For each FCOS head, in order to make features $\varphi_i(z)$ and $\varphi_i(x)$ better suited for classification and regression tasks, we adjust them to $\{[\varphi_i(z)]_{cls}, [\varphi_i(z)]_{reg}\}$ and $\{[\varphi_i(x)]_{cls}, [\varphi_i(x)]_{reg}\}$ by a convolutional layer. Then, each branch combines the adjusted features with Depthwise Cross Correlation operation (DW-XCorr) [23], which is formulated as

$$\begin{aligned} S_{w \times h \times 2} &= \psi_s([\varphi(z)]_{cls} \star [\varphi(x)]_{cls}), \\ R_{w \times h \times 4} &= \psi_r([\varphi(z)]_{reg} \star [\varphi(x)]_{reg}). \end{aligned} \quad (1)$$

where $S_{w \times h \times 2}$ and $R_{w \times h \times 4}$ represent the outputs of classification branch and regression branch, w, h denote width and height of the

output, ψ represents four 3×3 convolutional layers. In this way, we can learn a similarity match and achieve efficient information association of exemplar z and instance x in the embedding space. FCOS head is shown in Figure 3.

For the classification branch, we divide it into two sub-branches: a score map sub-branch for localization and a center-ness [39] sub-branch for the selection of a better bounding box. To obtain the labels of the score map, we map each pixel point (x, y) in the score map back to instance x according to the following relationship:

$$X = \lfloor \frac{s}{2} \rfloor + sx, \quad Y = \lfloor \frac{s}{2} \rfloor + sy. \quad (2)$$

where s represents the stride of Siamese network. If a point (X, Y) in the instance x falls into the ground-truth bounding box, whose corresponding point (x, y) in the score map is regarded as a positive sample and we set its label to 1. On the contrary, if the points fall outside the ground-truth bounding box, which are seen as negative samples. In short, it is a binary classification problem that distinguishes foreground from background. Figure 1 illustrates the mapping process and the selection of samples. Red points and white points represent positive samples and negative samples respectively.

For the regression branch, the output is a 4 channels feature map. As mentioned earlier, we adopt a per-pixel prediction fashion that each positive sample has the potential to generate a bounding box. Each positive sample corresponds to a 4D vector (l^*, t^*, r^*, b^*) that represents the distances from (X, Y) to four sides of the ground-truth bounding box in the instance x . The training regression targets can be formulated as:

$$\begin{aligned} l^* &= X - x_0, & t^* &= Y - y_0, \\ r^* &= X + x_1, & b^* &= Y - y_1. \end{aligned} \quad (3)$$

where (x_0, y_0) and (x_1, y_1) represent top-left and bottom-right coordinates of the ground-truth. Compared with the trackers based on RPN [23, 24] that regress the target bounding boxes with predefined anchor boxes as reference, our anchor-free method can directly predict bounding boxes and reduce hyper-parameters. Furthermore, because our approach uses pixel-level features that hardly bring about a wrong match between the score map and the regression output, our per-pixel prediction fashion is more suitable for the tracking task.

Although all of the positive samples and their corresponding 4D vectors can generate bounding boxes of the tracking target, there are still many low-quality predicted bounding boxes that should be suppressed. Otherwise, these bad bounding boxes may cause the degradation of localization accuracy. To select the boxes that have high IoU (Intersection of Union) with ground-truth, we add a new center-ness sub-branch that parallels with the score map sub-branch. The center-ness sub-branch is depicted as the normalized distance from the location to the center of the object. We simply implement it by a 1×1 convolutional layer. And the center-ness targets can be described as:

$$Centerness = \begin{cases} c, & \min(l^*, t^*, r^*, b^*) > 0 \\ 0, & otherwise \end{cases} \quad (4)$$

$$where \quad c = \sqrt{\frac{\min(l^*, r^*)}{\max(l^*, r^*)} \times \frac{\min(t^*, b^*)}{\max(t^*, b^*)}}. \quad (5)$$

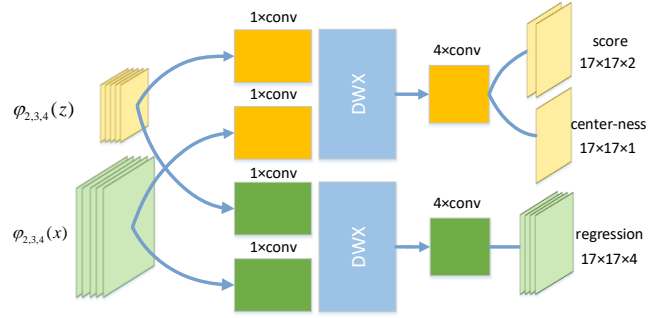


Figure 3: Details of FCOS head

In this way, the center-ness targets range from 0 to 1. For the positive samples in the score map, the smaller distances between the position of positive samples and the tracking target's center, the greater response that they can get in the center-ness map. We consider the points that close to the center of the target has a better regression effect. To some extent, the center-ness sub-branch can also alleviate the impact of partial occlusion. For the negative samples in the score map, they have no bounding box regression, so we simply set them to 0 in the center-ness target.

3.3 Hard Negative Samples Emphasis

We observe that many Siamese-based trackers are not discriminative for objects belonging to the same category, which leads to tracking failures of Siamese-based algorithms. To address this issue, we analyze the reasons leading to the problem and put forward our improvement.

Firstly, modern deep networks are introduced into the tracking community one after another [23, 50]. However, deep networks are pre-trained on ImageNet [21] for image classification. Because of rich semantic information, deep convolutional features are more beneficial for image classification. By contrast, shallow features contain low-level information and their high spatial resolution are more suitable for visual tracking. Siamese-based trackers simply use image pairs to fine-tune the networks. The output features contain most of the semantic information and ignore important detailed information to discriminate intra-class objects.

Secondly, there is no efficient method to constrain hard negative samples in the training phase. We classify samples on the instance x into three classes: positive samples, hard negative samples and easy negative samples. Hard negative samples are composed of cluster background and other similar objects. Existing tracking methods equally treat hard/easy negative samples, which makes them unable to distinguish hard negative samples and the performance is limited.

Based on the above analyses and inspired by person re-identification [45–47], we put forward our hard negative samples emphasis method to solve the aforementioned problem. Person re-identification is a task to find the same person across cameras, which commonly uses neural networks to extract embedding vectors that represent the appearance of that object. Then a distance metric is adopted to measure their similarity. For the tracking task, we intend to adopt the same idea to keep the discrimination of positive samples and hard negative samples. As illustrated in Figure 4, many sequences

of training sets contain hard negative samples that should be constrained in the training phase. To be specific, we first select related bounding boxes according to the score ranking in the score map. Non-Maximal Suppression (NMS) [35] is employed to eliminate redundant bounding boxes. In this way, we can obtain the candidate bounding boxes that include positive samples and hard negative samples. Specially, positive samples are defined as the candidates which have $IoU > T_h$ with the corresponding ground-truth. Hard negative ones are defined as the candidates which satisfy $IoU < T_l$. To avoid a bad training effect caused by the imbalance of positive samples and hard negative samples, we adopt a random shift operation of the ground-truth to generate positive samples. In this way, we can obtain high-quality RoIs in the instance x . In Figure 4, bounding boxes in yellow represent positive samples and the bounding boxes in white represent hard negative samples.

Considering that deeper features contain less detailed information, our goal is forcing deep features to keep the discrimination of positive samples and hard negative samples. After getting the selected bounding boxes, a RoI Align [13] layer crops the region on exemplar z or instance x , resulting in the output feature maps of a pre-determined size. For the exemplar branch of Siamese network, a RoI Align [13] layer takes the fused features $Cat(\varphi_3(z), \varphi_4(z))$ and the ground-truth bounding box as input, the output is the regional feature with the size of $5 \times 5 \times C$. Then two convolutional layers adjust it to a vector, namely *exemplar vector*. For the instance branch, we use the same way to generate *positive vectors* and *negative vectors*. Here we consider it as a recognition problem. By the constraint of the loss function, we intend to make the distance between *exemplar vector* and *positive vectors* as small as possible, meanwhile, the distances between *exemplar vector* and *negative vectors* are enabled to be as long as possible. A contrastive loss [10] is adopted here and formulated as follows:

$$L_{contra} = \frac{1}{N} \sum_{i=1}^N [y_i \cdot d_i^2 + (1 - y_i) \cdot \max(0, m - d_i)^2] \quad (6)$$

where d_i denotes the Euclidean distance between *exemplar vector* and *positive/negative vectors*, $y_i \in \{0, 1\}$ represents their corresponding labels. For positive vectors, we set $y_i = 1$, otherwise, $y_i = 0$. Here, m denotes a margin and is equal to 2. N is the number of selected RoIs.

3.4 Offline Training

The whole framework is composed of an anchor-free Siamese tracker and a hard negative samples emphasis network. We have already detailed anchor-free Siamese tracker in Section 3.2. For the classification branch, we adopt a focal loss [29] to restrain the score map, and train the center-ness map with a Binary Cross Entropy (BCE) loss. For the regression branch, the IoU loss [48] is employed which is formulated as:

$$L_{reg} = \frac{1}{N_p} \sum_{i=1}^{N_p} -\ln\left(\frac{P_i \cap G}{P_i \cup G}\right) \quad (7)$$

where P denotes the predicted bounding boxes and G denotes the ground-truth. N_p is the number of positive samples in the score map. \cap and \cup represent intersection operator and union operator



Figure 4: Illustration of hard negative samples in training datasets. Bounding boxes in red, yellow and white denote ground-truth, positive samples and hard negative samples respectively.

respectively. We optimize the final loss function as follows,

$$L = \lambda_1 L_{sco} + \lambda_2 L_{cen} + \lambda_3 L_{reg} + \lambda_4 L_{contra} \quad (8)$$

where L_{sco} is the focal loss [29] in charge of foreground-background classification, L_{cen} denotes a Binary Cross Entropy (BCE) for the center-ness map. L_{reg} represents the IoU loss [48] as shown in Eq. (7) and L_{contra} denotes the contrastive loss to enlarge the distances between positive vectors and hard negative vectors. The hyper-parameters are set to $\lambda_1 = \lambda_2 = \lambda_3 = 1, \lambda_4 = 0.1$.

3.5 Online Tracking

We first get the exemplar z from the first frame, which is not updated throughout the whole tracking process. Consequently, one branch of Siamese network takes the exemplar z as input. The instance x , which is cropped from the current frame, is taken as the input of another branch. As illustrated in Figure 2, there are three FCOS heads in the framework, we can obtain a score map (s), a center-ness map (c) and a regression (r) by each FCOS head. The output can be obtained by a weighted summation,

$$S = \sum_{i=2}^4 w_i^s \cdot s_i, \quad C = \sum_{i=2}^4 w_i^c \cdot c_i, \quad R = \sum_{i=2}^4 w_i^r \cdot r_i. \quad (9)$$

where w_i^s, w_i^c, w_i^r are trainable parameters. Then, we exert a softmax function in the score map (S) for foreground-background discrimination and perform an element-wise multiplication between the score map and the center-ness map to get the final score map. To penalize large displacements and suppress the large change in size and aspect ratio, we also exert a cosine window and a scale change penalty [24] to the final score map. The scale change penalty is formulated as:

$$penalty = \exp(k \cdot \max(\frac{r}{r'}, \frac{r'}{r}) \cdot \max(\frac{s}{s'}, \frac{s'}{s})). \quad (10)$$

where k is a hyper-parameter, r denotes the aspect ratio of the predicted bounding boxes in the current frame and r' is that in the previous frame, s is computed by

$$s = \sqrt{(w+p) \cdot (h+p)} \quad (11)$$

and s' is that in the previous frame, here w and h denote width and height of the target. p is equal to $(w+h)/2$. After that, the

coordinate of the highest score value in the final score map is exactly the position of the tracking target and is the position of the selected bounding box.

4 EXPERIMENTS

In this section, we first introduce the implementation details of our method. Then, we compare our approach with state-of-the-art trackers on six commonly used benchmark datasets, including GOT-10k [16], UAV123 [31], VOT2016 [18], VOT2018 [19], VOT2019 [20], LaSOT [8]. Finally, we perform ablation studies to demonstrate the effectiveness of our method.

4.1 Implementation Details

Data Preprocessing. We train the network on six large training datasets including YouTube-BB [33], COCO [30], ImageNet-VID [21], ImageNet-DET [21], GOT-10k [16], LaSOT [8]. The size of exemplar z is $127 \times 127 \times 3$ and the size of instance x is $255 \times 255 \times 3$. In order to eliminate the impact of the convolutional layers’ padding operation and simulate the real tracking scenarios, a random translation (± 64 pixel) is exerted to the target in the instance x . During training, we select pairs of cropped images that belong to the same sequences, and the interval of image pairs is less than 100 frames for ImageNet-VID [21], LaSOT [8], GOT-10k [16] and less than 3 frames for Youtube-BB [33]. Some data augmentation methods like scaling and color change are also employed for better training effect.

Training Details. We use a modified ResNet-50 [14] pre-trained on ImageNet [21] as our backbone. In the training stage, We train the model for 20 epochs with mini-batches of size 28. For the first 10 epochs, we freeze the parameters of backbone and only fine-tune the parameters of three FCOS [39] heads. For the last 10 epochs, the parameters of *block2*, *block3* and *block4* are unfrozen. The base learning rate is 5×10^{-3} and we use a warm-up learning rate of 10^{-3} for the first 5 epochs. For the last 15 epochs, the learning rate is decreased exponentially at each epoch from 5×10^{-3} to 5×10^{-4} . We train the network by stochastic gradient descent (SGD) with a weight decay of 10^{-4} and a momentum of 0.9. For hard negative samples emphasis method, the threshold of classifying positive samples and hard negative samples are set to $T_h = 0.8$ and $T_l = 0.3$. The threshold of NMS is equal to 0.7. Our training experiments are implemented using PyTorch on PC with an Intel i9-7900X and four NVIDIA Titan XP GPUs.

4.2 Results on GOT-10k

GOT-10k [16], which consists of 10,000 short sequences, is a large tracking database that offsets a wild converge of common moving objects in the wild. Huang et al. [16] select 180 videos to form the test subset for evaluation. They take average overlap (AO) and success rate (SR) as the performance indicators. AO denotes the average of overlaps between all ground-truth and estimated bounding boxes, while SR measures the percentage of successful tracked frames where the overlaps exceed a threshold ($SR_{0.5}$ and $SR_{0.75}$). For evaluation, all results are evaluated by the server provided by Huang et al. [16].

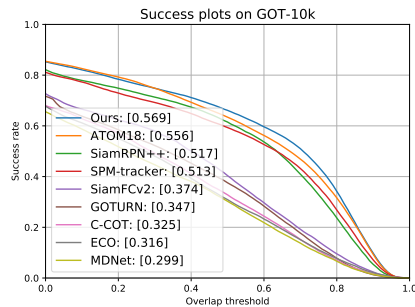


Figure 5: Comparison of state-of-the-art trackers on GOT-10k [16] in terms of success rate.

We can obtain outstanding performance on GOT-10k. Success plot is shown in Figure 5, and the detailed performance scores of trackers are illustrated in table 1. Our method can achieve AO score of 0.569, outperforming the second-best tracker ATOM [4] with a relative gain of 2.3% and exceeding the baseline method (SiamRPN++ [23]) by 10% improvement. As for the success rate, our tracker can get $SR_{0.5}$ and $SR_{0.75}$ scores of 0.661 and 0.439 while tracking with a real-time speed.

4.3 Results on VOT

Visual Object Tracking (VOT) dataset [19] consists of 60 challenging sequences and some sequences are updated annually. We usually evaluate the performance of trackers with the official VOT toolkit. The performance is evaluated in terms of accuracy (A) and robustness (R), which respectively denote the average overlap over successfully tracked frames and failure rate. Expected Average Overlap (EAO), which merges both accuracy and robustness, is always used to ranking test.

In table 2 and table 3, we report the experiment results on VOT2016 [18], VOT2018 [19] and VOT2019 [20]. Compared with state-of-the-art trackers, our method can get outstanding performance. For a fair comparison, our test environment is the same as SiamRPN++ [23]. On VOT2016, we can get EAO score of 0.487 that outperforms the baseline method SiamRPN++ [23] with a relative gain of 1.8% in terms of EAO. On VOT2018, the EAO score of our tracker is higher than SiamRPN++ [23] by 4.6%. Furthermore, on VOT2019, our method can surpass SiamRPN++ [23] in each indicators.

4.4 Results on UAV123

UAV123 [31] consists of 123 aerial video sequences comprising more than 110K frames, which takes precision and success rate as indicators for evaluation. The comparison of the proposed method with representative trackers (SiamRPN++ [23], DaSiamRPN [51], SiamRPN [24], SRDCF [6], SAMF [28], Struck [11], TLD [17]) is illustrated in Figure 6. We can see that our approach performs the two-best in this dataset in terms of precision and success rate. Our tracker achieves a precision score of 0.805 and a success score of 0.615, which are close to the best results.

Table 1: Performance comparisons on GOT-10k [16] benchmark. AO: average overlap; SR: success rate with different thresholds of 0.5 and 0.75. The best two results are highlighted in red and blue respectively.

Trackers	MDNet [32]	ECO [5]	CCOT [7]	GOTURN [15]	SiamFCv2 [1]	SPM-traker [41]	SiamRPN++ [23]	ATOM [4]	Ours
AO \uparrow	0.299	0.316	0.325	0.347	0.348	0.513	0.517	0.556	0.569
SR _{0.5} \uparrow	0.303	0.309	0.328	0.375	0.353	0.593	0.615	0.634	0.661
SR _{0.75} \uparrow	0.099	0.111	0.107	0.124	0.098	0.359	0.329	0.402	0.439

Table 2: Comparison of state-of-the-art trackers on VOT2016 [18] and VOT2018 [19] in terms of Accuracy, Robustness, EAO and speed. The best two results are highlighted in red and blue respectively.

Trackers	VOT2016			VOT2018			FPS
	A \uparrow	R \downarrow	EAO \uparrow	A \uparrow	R \downarrow	EAO \uparrow	
ECO[5]	0.54	0.20	0.374	0.484	0.276	0.280	8
SiamVGG[27]	0.564	-	0.351	0.531	0.318	0.286	33
SA_Siam_R[12]	0.54	-	0.291	0.566	0.258	0.337	50
TADT[26]	0.55	-	0.299	-	-	-	33.7
C-RPN[9]	0.594	-	0.363	-	-	0.289	36
SiamDW-rpn[50]	-	-	0.376	-	-	0.294	-
SiamRPN[24]	0.56	0.26	0.344	0.49	0.46	0.244	200
SPM-Tracker[41]	0.62	0.21	0.434	0.58	0.30	0.338	120
UPDT[2]	-	-	-	0.536	0.184	0.378	86
DaSiamRPN[51]	0.61	0.22	0.411	0.586	0.276	0.383	160
LADCF[44]	-	-	-	0.503	0.159	0.389	-
ATOM[4]	-	-	-	0.590	0.204	0.401	30
SiamRPN++[23]	0.637	0.177	0.478	0.600	0.234	0.414	35
Ours	0.635	0.158	0.487	0.596	0.183	0.433	37

Table 3: Comparison of state-of-the-art trackers on VOT2019 [20] in terms of EAO, Accuracy and Robustness.

Trackers	SA_Siam_R	SPM	SiamRPN++	SiamMask	Ours
EAO \uparrow	0.253	0.275	0.285	0.287	0.303
A \uparrow	0.559	0.577	0.599	0.594	0.600
R \downarrow	0.492	0.507	0.482	0.461	0.391

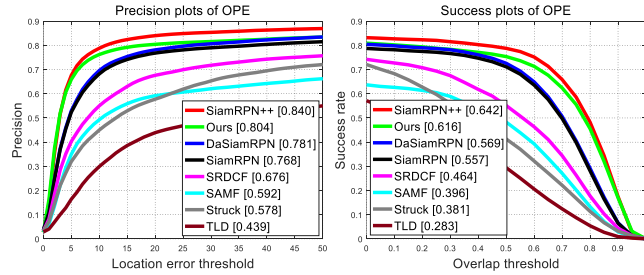


Figure 6: Comparisons with state-of-the-art tracking approaches on UAV123 [31] in terms of precision and success rate.

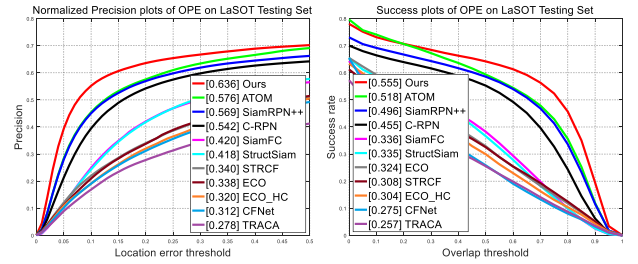


Figure 7: Comparison of state-of-the-art trackers on LaSOT [8] in terms of normalized precision and success rate.

4.5 Results on LaSOT

The Large-scale Single Object Tracking dataset (LaSOT) [8] is composed of 1,400 sequences and more than 3.5M frames that are labeled with high-quality dense annotations including 70 categories. The test subset of LaSOT contain 280 long-term videos. The average frame length of this dataset is more than 2,500 frames, so the evaluation results are convincing and truly reflect the performance of various trackers. LaSOT takes normalized precision and success rate as indicators for evaluation. Our algorithm is compared with other 14 trackers (SiamRPN++ [23], ATOM [4], C-RPN [9], SiamFC [1], StructSiam [49], ECO [5], CFNet [40], TRACA [3], STRCF [25]). The normalized precision plot and success plot are illustrated in Figure 7. Our tracker performs significantly better than the baseline model (SiamRPN++ [23]) by almost 11.7% in normalized precision and 11.8% in success.

4.6 Ablation Experiment

Analysis of hard negative samples emphasis: We evaluate our approach in different situations. Table 4 shows the results using GOT-10k [16] dataset under the measure of three key performance indicators. In the first column of table 4, ‘Baseline’ represents our baseline method SiamRPN++ [23]. ‘Ours w/o HE’ denotes the original model without hard negative samples emphasis and ‘Ours’ represents the complete model that we put forward. Table 4 demonstrates ‘Ours w/o HE’ outperforms ‘Baseline’ with a relative gain of 5.4% in terms of AO. By adding hard negative samples emphasis method, we improve the AO score on GOT-10K from 0.545 to 0.569. Furthermore, we select some representative sequences with hard negative samples from VOT2018 [19] and visualise their score maps. As shown in Figure 8. Obviously, the score map of ‘Ours’ shows better discriminability than that of ‘Ours w/o HE’.

Impact of the selected RoIs’ number: We have performed an ablation study on different numbers of RoIs. These selected RoIs

Table 4: ablation experiment on GOT-10k [16]

	AO \uparrow	SR $_{0.5}\uparrow$	SR $_{0.75}\uparrow$
Baseline	0.517	0.615	0.329
Ours w/o HE	0.545	0.638	0.388
Ours	0.569	0.661	0.439

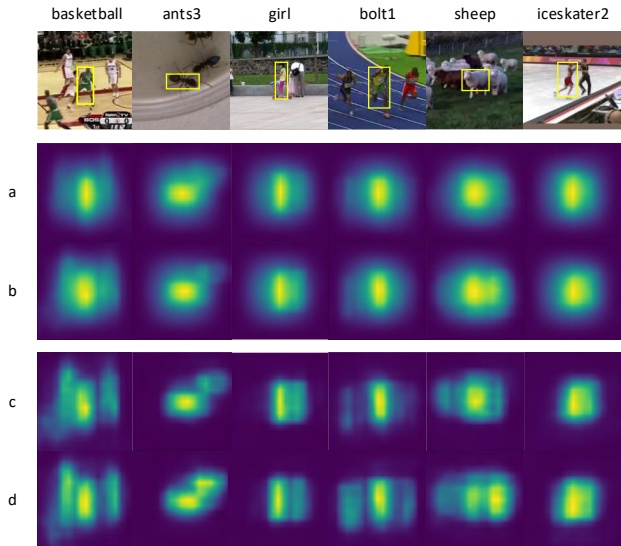


Figure 8: Visualization of score maps. The first row shows the original images of sequences. And (a) and (b) denote final score maps with penalty, (c) and (d) show score maps without penalty, (a) and (c) represent our model with hard negative samples emphasis. Bounding boxes in yellow denote tracking targets.

Table 5: Influence of the number of RoIs

RoIs' number	AO \uparrow	SR $_{0.5}\uparrow$	SR $_{0.75}\uparrow$
5	0.548	0.642	0.401
11	0.569	0.661	0.439
21	0.556	0.648	0.432
31	0.538	0.631	0.385

include k bounding boxes of positive samples, k bounding boxes of hard negative samples and one ground-truth bounding box. As shown in Table 5, we can get the best result when the number of RoIs is equal to 11. If there are too many selected RoIs, the performance of trackers will decrease.

5 CONCLUSIONS

In this paper, we perform a novel bounding box prediction framework with a per-pixel prediction fashion to train Siamese network for visual tracking. Compared with trackers based on RPN, our anchor-free approach can generate a more precise bounding box and reduce the number of hyper-parameters. Furthermore, we have a deep analysis of the tracking failure caused by hard negative

samples and propose a hard negative samples emphasis method to improve the discriminative power of Siamese networks. The evaluation results on frequently-used tracking benchmarks demonstrate that our proposed tracker can improve the performance and achieve real-time tracking.

ACKNOWLEDGMENTS

This work was supported by the National Science Fund of China under Grants (61771079) and Chongqing Youth Talent Program.

REFERENCES

- [1] Luca Bertinetto, Jack Valmadre, Joao F Henriques, Andrea Vedaldi, and Philip HS Torr. 2016. Fully-convolutional siamese networks for object tracking. In *European conference on computer vision*. Springer, 850–865.
- [2] Goutam Bhat, Joakim Johnander, Martin Danelljan, Fahad Shahbaz Khan, and Michael Felsberg. 2018. Unveiling the power of deep tracking. In *Proceedings of the European Conference on Computer Vision (ECCV)*. 483–498.
- [3] Jongwon Choi, Hyung Jin Chang, Tobias Fischer, Sangdoon Yun, and Young Choi Jin. 2018. Context-Aware Deep Feature Compression for High-Speed Visual Tracking. In *IEEE Conference on Computer Vision and Pattern Recognition*.
- [4] Martin Danelljan, Goutam Bhat, Fahad Shahbaz Khan, and Michael Felsberg. 2019. Atom: Accurate tracking by overlap maximization. In *Proceedings of the IEEE Conference on Computer Vision and Pattern Recognition*. 4660–4669.
- [5] Martin Danelljan, Goutam Bhat, Fahad Shahbaz Khan, and Michael Felsberg. 2017. Eco: Efficient convolution operators for tracking. In *Proceedings of the IEEE conference on computer vision and pattern recognition*. 6638–6646.
- [6] Martin Danelljan, Gustav Hager, Fahad Shahbaz Khan, and Michael Felsberg. 2015. Learning spatially regularized correlation filters for visual tracking. In *Proceedings of the IEEE international conference on computer vision*. 4310–4318.
- [7] Martin Danelljan, Andreas Robinson, Fahad Shahbaz Khan, and Michael Felsberg. 2016. Beyond correlation filters: Learning continuous convolution operators for visual tracking. In *European conference on computer vision*. Springer, 472–488.
- [8] Heng Fan, Liting Lin, Fan Yang, Peng Chu, Ge Deng, Sijia Yu, Hexin Bai, Yong Xu, Chunyuan Liao, and Haibin Ling. 2019. Lasot: A high-quality benchmark for large-scale single object tracking. In *Proceedings of the IEEE Conference on Computer Vision and Pattern Recognition*. 5374–5383.
- [9] Heng Fan and Haibin Ling. 2019. Siamese cascaded region proposal networks for real-time visual tracking. In *Proceedings of the IEEE Conference on Computer Vision and Pattern Recognition*. 7952–7961.
- [10] Raia Hadsell, Sumit Chopra, and Yann LeCun. 2006. Dimensionality reduction by learning an invariant mapping. In *2006 IEEE Computer Society Conference on Computer Vision and Pattern Recognition (CVPR'06)*, Vol. 2. IEEE, 1735–1742.
- [11] Sam Hare, Stuart Golodetz, Amir Saffari, Vibhav Vineet, Ming-Ming Cheng, Stephen L Hicks, and Philip HS Torr. 2015. Struck: Structured output tracking with kernels. *IEEE transactions on pattern analysis and machine intelligence* 38, 10 (2015), 2096–2109.
- [12] Anfeng He, Chong Luo, Xinmei Tian, and Wenjun Zeng. 2018. A twofold siamese network for real-time object tracking. In *Proceedings of the IEEE Conference on Computer Vision and Pattern Recognition*. 4834–4843.
- [13] Kaiming He, Georgia Gkioxari, Piotr Dollár, and Ross Girshick. 2017. Mask r-cnn. In *Proceedings of the IEEE international conference on computer vision*. 2961–2969.
- [14] Kaiming He, Xiangyu Zhang, Shaoqing Ren, and Jian Sun. 2016. Deep residual learning for image recognition. In *Proceedings of the IEEE conference on computer vision and pattern recognition*. 770–778.
- [15] David Held, Sebastian Thrun, and Silvio Savarese. 2016. Learning to track at 100 fps with deep regression networks. In *European Conference on Computer Vision*. Springer, 749–765.
- [16] Lianghua Huang, Xin Zhao, and Kaiqi Huang. 2019. Got-10k: A large high-diversity benchmark for generic object tracking in the wild. *IEEE Transactions on Pattern Analysis and Machine Intelligence* (2019).
- [17] Zdenek Kalal, Krystian Mikolajczyk, and Jiri Matas. 2011. Tracking-learning-detection. *IEEE Trans Pattern Anal Mach Intell* 34, 7 (2011), 1409–1422.
- [18] Matej Kristan, Aleš Leonardis, Jiri Matas, Michael Felsberg, Roman Pflugfelder, Luka Čehovin Zajc, Tomas Vojir, Gustav Häger, Alan Lukežič, and Gustavo Fernandez. 2016. The Visual Object Tracking VOT2016 challenge results. Springer. <http://www.springer.com/gp/book/9783319488806>
- [19] Matej Kristan, Ales Leonardis, Jiri Matas, Michael Felsberg, Roman Pflugfelder, Luka Čehovin Zajc, Tomas Vojir, Goutam Bhat, Alan Lukežic, Abdelrahman Eldesokey, Gustavo Fernandez, and et al. 2018. The sixth Visual Object Tracking VOT2018 challenge results.
- [20] Matej Kristan, Jiri Matas, Ales Leonardis, Michael Felsberg, Roman Pflugfelder, Joni-Kristian Kamarainen, Luka Čehovin Zajc, Ondrej Drbohlav, Alan Lukežic,

- Amanda Berg, Abdelrahman Eldesokey, Jani Kapyla, and Gustavo Fernandez. 2019. The Seventh Visual Object Tracking VOT2019 Challenge Results.
- [21] Alex Krizhevsky, Ilya Sutskever, and Geoffrey E Hinton. 2012. Imagenet classification with deep convolutional neural networks. In *Advances in neural information processing systems*. 1097–1105.
- [22] Hei Law and Jia Deng. 2018. Cornernet: Detecting objects as paired keypoints. In *Proceedings of the European Conference on Computer Vision (ECCV)*. 734–750.
- [23] Bo Li, Wei Wu, Qiang Wang, Fangyi Zhang, Junliang Xing, and Junjie Yan. 2019. Siamrpn++: Evolution of siamese visual tracking with very deep networks. In *Proceedings of the IEEE Conference on Computer Vision and Pattern Recognition*. 4282–4291.
- [24] Bo Li, Junjie Yan, Wei Wu, Zheng Zhu, and Xiaolin Hu. 2018. High performance visual tracking with siamese region proposal network. In *Proceedings of the IEEE Conference on Computer Vision and Pattern Recognition*. 8971–8980.
- [25] Feng Li, Cheng Tian, Wangmeng Zuo, Lei Zhang, and Ming-Hsuan Yang. 2018. Learning spatial-temporal regularized correlation filters for visual tracking. In *Proceedings of the IEEE Conference on Computer Vision and Pattern Recognition*. 4904–4913.
- [26] Xin Li, Chao Ma, Baoyuan Wu, Zhenyu He, and Ming-Hsuan Yang. 2019. Target-aware deep tracking. In *Proceedings of the IEEE Conference on Computer Vision and Pattern Recognition*. 1369–1378.
- [27] Yuhong Li and Xiaofan Zhang. 2019. SiamVGG: Visual tracking using deeper siamese networks. *arXiv preprint arXiv:1902.02804* (2019).
- [28] Yang Li and Jianke Zhu. 2014. A scale adaptive kernel correlation filter tracker with feature integration. In *European conference on computer vision*. Springer, 254–265.
- [29] Tsung-Yi Lin, Priya Goyal, Ross Girshick, Kaiming He, and Piotr Dollár. 2017. Focal loss for dense object detection. In *Proceedings of the IEEE international conference on computer vision*. 2980–2988.
- [30] Tsung-Yi Lin, Michael Maire, Serge Belongie, James Hays, Pietro Perona, Deva Ramanan, Piotr Dollár, and C Lawrence Zitnick. 2014. Microsoft coco: Common objects in context. In *European conference on computer vision*. Springer, 740–755.
- [31] Matthias Mueller, Neil Smith, and Bernard Ghanem. 2016. A benchmark and simulator for uav tracking. In *European conference on computer vision*. Springer, 445–461.
- [32] Hyeonseob Nam and Bohyung Han. 2016. Learning multi-domain convolutional neural networks for visual tracking. In *Proceedings of the IEEE conference on computer vision and pattern recognition*. 4293–4302.
- [33] Esteban Real, Jonathon Shlens, Stefano Mazzocchi, Xin Pan, and Vincent Vanhoucke. 2017. Youtube-boundingboxes: A large high-precision human-annotated data set for object detection in video. In *Proceedings of the IEEE Conference on Computer Vision and Pattern Recognition*. 5296–5305.
- [34] Joseph Redmon, Santosh Divvala, Ross Girshick, and Ali Farhadi. 2016. You only look once: Unified, real-time object detection. In *Proceedings of the IEEE conference on computer vision and pattern recognition*. 779–788.
- [35] Shaoqing Ren, Kaiming He, Ross Girshick, and Jian Sun. 2015. Faster r-cnn: Towards real-time object detection with region proposal networks. In *Advances in neural information processing systems*. 91–99.
- [36] Karen Simonyan and Andrew Zisserman. 2014. Very deep convolutional networks for large-scale image recognition. *arXiv preprint arXiv:1409.1556* (2014).
- [37] Christian Szegedy, Wei Liu, Yangqing Jia, Pierre Sermanet, Scott Reed, Dragomir Anguelov, Dumitru Erhan, Vincent Vanhoucke, and Andrew Rabinovich. 2015. Going deeper with convolutions. In *Proceedings of the IEEE conference on computer vision and pattern recognition*. 1–9.
- [38] Ran Tao, Efstratios Gavves, and Arnold WM Smeulders. 2016. Siamese instance search for tracking. In *Proceedings of the IEEE conference on computer vision and pattern recognition*. 1420–1429.
- [39] Zhi Tian, Chunhua Shen, Hao Chen, and Tong He. 2019. Fcos: Fully convolutional one-stage object detection. In *Proceedings of the IEEE International Conference on Computer Vision*. 9627–9636.
- [40] Jack Valmadre, Luca Bertinetto, Joao Henriques, Andrea Vedaldi, and Philip HS Torr. 2017. End-to-end representation learning for correlation filter based tracking. In *Proceedings of the IEEE Conference on Computer Vision and Pattern Recognition*. 2805–2813.
- [41] Guangting Wang, Chong Luo, Zhiwei Xiong, and Wenjun Zeng. 2019. Spm-tracker: Series-parallel matching for real-time visual object tracking. In *Proceedings of the IEEE Conference on Computer Vision and Pattern Recognition*. 3643–3652.
- [42] Y. Wu, J. Lim, and M. Yang. 2013. Online Object Tracking: A Benchmark. In *2013 IEEE Conference on Computer Vision and Pattern Recognition*. 2411–2418.
- [43] Y. Wu, J. Lim, and M. Yang. 2015. Object Tracking Benchmark. *IEEE Transactions on Pattern Analysis and Machine Intelligence* 37, 9 (2015), 1834–1848.
- [44] Tianyang Xu, Zhen-Hua Feng, Xiao-Jun Wu, and Josef Kittler. 2019. Learning Adaptive Discriminative Correlation Filters via Temporal Consistency Preserving Spatial Feature Selection for Robust Visual Object Tracking. *IEEE Transactions on Image Processing* 28, 11 (2019), 5596–5609.
- [45] Xun Yang, Meng Wang, Richang Hong, Qi Tian, and Yong Rui. 2017. Enhancing person re-identification in a self-trained subspace. *ACM Transactions on Multimedia Computing, Communications, and Applications (TOMM)* 13, 3 (2017), 1–23.
- [46] Xun Yang, Meng Wang, and Dacheng Tao. 2017. Person re-identification with metric learning using privileged information. *IEEE Transactions on Image Processing* 27, 2 (2017), 791–805.
- [47] Xun Yang, Peicheng Zhou, and Meng Wang. 2018. Person reidentification via structural deep metric learning. *IEEE Transactions on Neural Networks and Learning Systems* 30, 10 (2018), 2987–2998.
- [48] Jiahui Yu, Yuning Jiang, Zhangyang Wang, Zhimin Cao, and Thomas Huang. 2016. Unitbox: An advanced object detection network. In *Proceedings of the 24th ACM international conference on Multimedia*. 516–520.
- [49] Yunhua Zhang, Lijun Wang, Jinqing Qi, Dong Wang, Mengyang Feng, and Huchuan Lu. 2018. Structured siamese network for real-time visual tracking. In *Proceedings of the European conference on computer vision (ECCV)*. 351–366.
- [50] Zhipeng Zhang and Houwen Peng. 2019. Deeper and wider siamese networks for real-time visual tracking. In *Proceedings of the IEEE Conference on Computer Vision and Pattern Recognition*. 4591–4600.
- [51] Zheng Zhu, Qiang Wang, Bo Li, Wei Wu, Junjie Yan, and Weiming Hu. 2018. Distractor-aware siamese networks for visual object tracking. In *Proceedings of the European Conference on Computer Vision (ECCV)*. 101–117.